PAPER

Reaction contest: hydrolysis *versus* intramolecular cyclisation reaction in alkyl squaramate esters†

Marta Ximenis, [ID] Santiago Cañellas, [ID] Rosa M. Gomila, [ID] Bartomeu Galmés, Antonio Frontera, [ID] Antonio Costa [ID] and Carmen Rotger [ID] *

The stability and hydrolytic behavior of squaramate esters in aqueous solutions have been investigated. The structure of squaramates and the nature of adjacent groups significantly influence their aqueous stability and reactivity towards nucleophiles. Squaramate esters, lacking or containing weakly basic neighboring group participation (NGP) substitutions, remain stable up to pH 9. Their hydrolysis rate ($k_{OH} \approx 10^{-1}$ M^{-1} s^{-1}) is 1000 times faster than that of squaramides, following a second-order rate law. Squaramate esters functionalized with basic NGP groups, such as amines, display a pH-dependent hydrolysis rate due to anchimeric assistance of the terminal amino group, reducing stability to pH 5. However, when the squaramate ester has a terminal nucleophilic group in the γ position of the alkyl chain, it undergoes rapid intramolecular cyclization, forming cyclic squaramides.

Introduction

Alkyl squaramates, the 3-amino, 4-alkoxy derivatives of squaric acid, are directly synthesised from squaramate diesters by condensation with amines.[1] This reaction, typically conducted at room temperature, without catalyst or coupling reagents has drawn much attention due to its straightforward protocols and high yields.[2]

Squaric acid esters have emerged as valuable tools for synthesising compounds with diverse applications, including dyes,[3–5] catalysts,[6,7] sensors,[8–12] anion transporters,[13–17] and bioactive compounds.[18–21] In general, their reactivity with primary or secondary amines and a certain resistance to hydrolysis makes them suitable for preparing amino-saccharide, protein, and nucleic acid conjugates with significant biomedical applications,[22] such as neoglycoproteins for cell targeting,[23] synthetic vaccines,[24] and lectin recognition[2,25] among others. Furthermore, squaric acid esters modify proteins through highly chemoselective reactions with the amino acid cysteine.[26,27]

However, despite the widespread use of squaric esters, understanding their fate and degradation pathways in biological-like environments remains limited. Unlike squaramides, which exhibit kinetic stability for more than 100 days in the pH range of 3–10 at 37 °C, squaramate esters suffer hydrolysis under milder conditions.[28] Studies have shown that the

hydrolysis of squaramate alkyl esters occurs over days at pH 9, with greater stability observed for longer alkyl chains.[29]

Additionally, the influence of Neighbouring Group Participation (NGP) on the kinetics of various reactions has been well-documented.[30,31] Specifically, the hydrolysis of carboxylic esters is enhanced by the NGP through the formation of a cyclic intermediate.[32,33] Similar behaviour is anticipated for squaramate esters. However, an intramolecular cyclisation reaction, driven by a nucleophilic attack from a group of the squaramate substituent, might compete with the hydrolysis, Chart 1.

The distinctive conformational properties of squaric acid derivatives could play a key role in this context. Previous studies have demonstrated that these conformational properties of secondary and tertiary squaramate esters facilitate a rapid intramolecular cyclisation reaction through the nucleophilic attack of a group located at the γ position of the squaramide substituent.[34,35]

This study investigates the kinetic competition between hydrolysis and intramolecular cyclisation reactions in squaramate esters. We examine the effect of NGP on the hydrolysis rate and the role of different nucleophiles (N, S) in the cyclisation reaction, using a primary amine and a thiol group to mimic the behaviour of the amino acids lysine and cysteine, respectively, in peptide or protein bioconjugation.
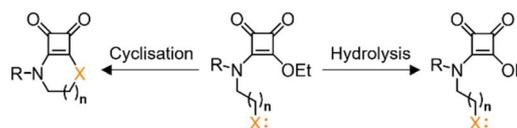
Universitat de les Illes Balears, Cra. Valldemossa Km 7.5, Palma de Mallorca, 07122, Spain. E-mail: carmen.rotger@uib.es

† Electronic supplementary information (ESI) available: General information, experimental details, characterization data for products, NMR spectra of products, and cartesian coordinates of computed structures. See DOI: https://doi.org/10.1039/d4ra04362f

Chart 1 Hydrolysis *vs.* intramolecular cyclisation pathways for squaramate esters.
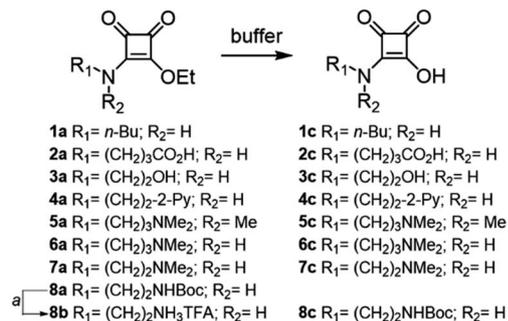
Fig. 1 Structure of the squaramate esters **1a–8b** and the corresponding squaramic acids **1c–8c** obtained from their buffered hydrolysis at 37 °C. [a]TFA in CH_2Cl_2.

First, we investigated the hydrolysis reaction in squaramate ethyl esters. Similar to carboxylic esters, we assumed that the hydrolysis of squaramate esters would proceed under both acid and alkaline catalysis (see Scheme S1†).

Therefore, we synthesized squaramate esters **1a–7a** and **8b** to assess the hydrolytic stability within the pH range of 3 to 9, Fig. 1. The structure of the studied esters differs from the nature of the *N*-alkyl chain. Compounds **2a–7a** and **8b** were functionalized with chemical groups that potentially assist the hydrolytic reaction (amine, carboxyl, alcohol, and pyridine groups). Compound **1a** featuring an *n*-butyl chain, served as a negative control for NGP.

Squaramate esters **1a–8a** were synthesised by condensing diethyl squarate with one equivalent of the corresponding amine in acetonitrile (see ESI†). The amino-protecting group of compound **8a** was cleaved with trifluoroacetic acid (TFA) in dichloromethane to yield the corresponding ammonium salt **8b**.

The kinetics of the hydrolysis of compounds **1a–7a** and **8b** to give the corresponding squaramic acids **1c–8c** were studied by UV-spectroscopy. In aqueous solution, squaramic esters exhibit a strong absorption UV band ($\varepsilon > 6 \times 10^4$ M^{-1} cm^{-1}) with a maximum at 272 nm, independent of the pH, while the squaramate acid derivatives display a maximum absorption band at 283 nm. Capitalizing on this, we monitored the time-dependent changes in the UV-vis spectra of esters **1a–7a** and **8b** at 37 °C to mimic physiological conditions, Fig. 2a. The experiments were conducted under pseudo-first-order conditions, and the apparent rate constants (k_{obs}) were determined through global absorption spectra analysis‡ (see ESI eqn (2′)†).

The calculated k_{obs} values are summarized in Table 1. Based on these data, the squaramate esters studied can be classified into two groups.

The first group comprises esters **1a–4a**, which exhibit kinetic stability under pH 9, and the second group includes esters **5a–7a** and **8b**, undergoing hydrolysis from pH 7 onwards. Noticeably, at pH 9, the hydrolysis for esters **5a–7a** and **8b** occurs significantly faster compared to esters **1a–4a**, highlighting the role of the basic NGPs on the reaction kinetics.

‡ Data vas fitted using ReactLabTM Kinetics (Jplus Consulting Ltd) software package.
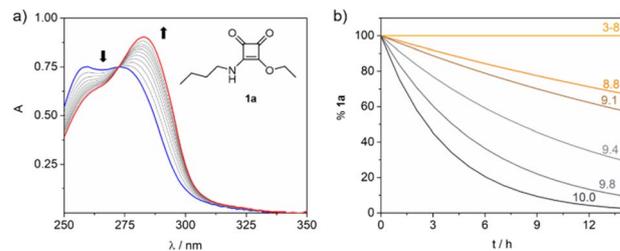

Fig. 2 (a) Changes observed in the UV spectra of **1a** (blue trace) due to hydrolysis (30 µM in 10 mM carbonate buffer, pH 10, 37 °C) as a representative example of the studied squaramate esters. Red trace represents the corresponding hydrolysed squaric acid. (b) Calculated disappearance of **1a** (30 µM, 37 °C) from the UV spectrum at different pH (10 mM carbonate buffer). From pH 3 to 8, no hydrolysis was observed after one week.

Table 1 Pseudo-first order observed rate contents for the hydrolysis of squaramate esters **1a–7a** and **8b** at different pH (3–9). k_{obs} 10^{-5} s^{-1}

	pH				
	3	5	7	8	9
1a	—	—	—	—	1.10 ± 0.04
2a	—	—	—	—	0.34 ± 0.03
3a	—	—	—	—	0.86 ± 0.01
4a	—	—	—	—	0.73 ± 0.04
5a	—	—	0.02 ± 0.01	0.43 ± 0.03	3.62 ± 0.02
6a	—	—	0.31 ± 0.01	1.03 ± 0.01	4.85 ± 0.02
7a	—	—	0.46 ± 0.01	2.38 ± 0.03	8.56 ± 0.14
8b	—	—	1.01 ± 0.01	2.91 ± 0.01	16.1 ± 0.2

Ester **1a** hydrolysis was further examined under pseudo-first-order conditions (3×10^{-5} M and 37 °C) at the pH range of 8.8–10, as illustrated in Fig. 2b. In contrast to observations in acidic or neutral media, the hydrolysis of **1a** occurs within hours under alkaline conditions, yielding acid **1c**. The obtained k_{obs} values show a linear dependence within the pH range studied. This linear relationship discards the ionization of the squaramidic NH within this pH interval, as such ionization would lead to a non-linear dependence of the obtained k_{obs}. From the data fitting, we could calculate a second-order rate constant k_{OH} of 0.47 ± 0.02 M^{-1} s^{-1} for the hydrolysis reaction.[36]

The same linear dependency was observed when conducting the aforementioned experiments in a D_2O solution of **1a** (3×10^{-5} M, pD 9.1–10.2, 37 °C), obtaining a value of k_{OD} of 0.21 ± 0.02 M^{-1} s^{-1}. The solvent Kinetic Isotope Effect (KIE) calculated as k_{OH}/k_{OD} was found to be 2.24 ± 0.02 falling within the typical range of 1.5–3 that corresponds to solvent KIEs resulting from the transfer of a proton from nitrogen or oxygen atoms (see Fig. S3†).[37] Therefore, the obtained KIE value supports the involvement of a water molecule in the rate-determining step (RDS) of the reaction. These results align with the proposed general base-catalysed mechanism for the hydrolysis of carboxylic esters, suggesting that an analogous mechanism operates for the hydrolysis of the squaramate ester **1a** (see ESI Scheme S1†).
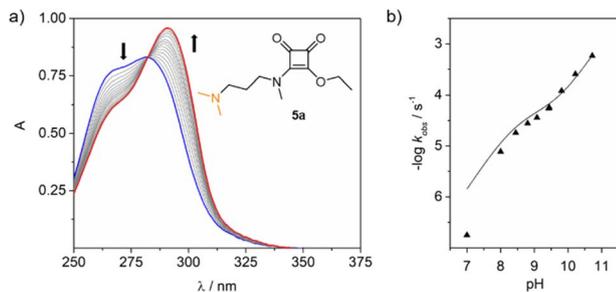
Fig. 3 (a) UV changes observed for the hydrolysis of ester **5a** (30 μM) at pH 9 (10 mM borate buffer) and 37 °C. (b) Data fitting to obtain k_1 and k_{OH}.

Table 2 Calculated rate constants for the assisted hydrolysis k_1 and direct hydrolysis k_{OH} reactions of esters **5a–7a** and **8a** and the pK_a values used for the constants fitting

	p$K_a{}^a$	k_{OH}, M^{-1} s^{-1}	k_1, 10^{-5} M^{-1} s^{-1}
5a	8.82	1.03 ± 0.04	5.2 ± 0.9
6a	8.61	1.03^b	12 ± 2
7a	7.95	1.03^b	3.9 ± 0.3
8b	8.50	1.03^b	30 ± 6

^{a} Obtained by potentiometric titration and fitted with Hyperquad2013 (Protonic Software. http://www.hyperquad.co.uk). To calculate k_1 we assumed the same k_{OH} found for **5a**. ^{b} To calculate k_1, we assumed the same k_{OH} as for **5a**.

In analogy to ester **1a** and assuming the same reactivity, we conducted the kinetic studies for **2a–4a** at the same pH interval as **1a** and fitted the data to obtain the corresponding constants $k_{(OH)}$. The fitted values of 0.34 ± 0.03 M^{-1} s^{-1} for **2a**, 0.86 ± 0.01 M^{-1} s^{-1} for **3a**, and 0.73 ± 0.04 M^{-1} s^{-1} for **4a** all fall within the same order of magnitude than the $k_{(OH)}$ obtained for **1a**. This indicates that the presence of poor nucleophilic/basic groups does not enhance the reaction rate when compared to **1a**. Thus, in this scenario, hydrolysis is likely governed solely by the electrophilic character of the squaryl ester carbon.

Similar to esters **1a–4a**, we observed that compounds **5a–7a** and **8a** withstand hydrolysis in moderate acidic media (pH 3–5, 37 °C) for over three weeks. However, their notably accelerated hydrolysis in neutral or alkaline media (7–10.5) at 37 °C suggests that the amine group on the *N*-alkyl chain could act as anchimeric assistance (NGP), thereby enhancing the hydrolysis reaction rate. We assumed that the terminal alkyl amine group would participate in an *N*-protonation equilibrium in water, where only the free amino group would be available to catalyse the reaction. Therefore, the hydrolysis would be sensitive to the pH.

$$k_{obs} = k_c[\text{I}] = k_c \frac{K_a{}'}{K_a{}' + [\text{H}]} \qquad (1)$$

To confirm our hypothesis, we ran the kinetic experiments on ester **5a** within the pH range of 7 to 10.5 at 37 °C, Fig. 3. Data fitting provided the corresponding k_{obs} for each pH studied. The rate constant k_1 found for the assisted hydrolysis is $5.2 \pm 0.9 \times 10^{-5}$ M^{-1} s^{-1}, and the rate constant for the direct hydrolysis k_{OH} is 1.03 ± 0.04 M^{-1} s^{-1}. Despite the calculated k_1 value being five orders of magnitude smaller than k_{OH}, it significantly contributes to the hydrolysis rate, particularly with increasing pH, where both proposed mechanisms operate simultaneously.

Consequently, we hypothesised that the rate law for the reaction would depend on the amine pK_a (eqn (1)), and the direct hydrolysis would compete with the NGP process.§

Similarly, we calculated the kinetic constant k_1 for squaramate esters **6a–7a** and **8b** using the k_{OH} value obtained for **5a** in

the fitting. The calculated k_1 values are listed in Table 2 and are within the same order of magnitude as that determined for **5a**, indicating the involvement of both primary and secondary amines as an NGP and thereby increasing the overall hydrolysis reaction rate.

In line with these results, a similar behaviour has been reported for carboxylic ester analogues. Mautner and Bruice studied the hydrolytic stability of the benzoyl choline ester at 25 °C, showing a kinetic profile akin to that found for compound **1a** (k_{OH} 0.56 M^{-1} s^{-1}), discarding the assistance of the tetraalkyl ammonium group to the hydrolysis reaction.[38] However, the hydrolytic constants obtained for the 2-(dimethylamino)ethyl benzoate ($k_{OH} = 0.06$ M^{-1} s^{-1} and $k_1 = 4.8 \times 10^{-5}$ M^{-1} s^{-1}) show faster hydrolysis like in compounds **5a–7a** and **8b**, due to the intramolecular assistance of the amino-terminal group. Our results suggest that squaramate esters exhibit moderate resistance to hydrolysis compared to their carboxylic analogs. In comparison with carbamates, squaramate esters like **1a** hydrolyse more rapidly under neutral and basic conditions. However, under acidic conditions, squaramate esters exhibit high stability, with no observable reaction over several days, while carbamate ester analogs hydrolyze within a few hours. Conversely, squaramate esters undergo hydrolysis around 1000 times faster than squaramides, mirroring the behavior observed in carboxylic acids and their corresponding amides.

After studying the hydrolysis of squaramate esters **1a–8b**, we delved into the competition of the intramolecular cyclisation reaction and the hydrolysis reaction to ascertain whether the intramolecular cyclization occurs more rapidly than the hydrolysis. To explore this further, we analysed the kinetic behaviour of squaramate esters **9a–10b**, whose structure could potentially yield cyclic squaramide compounds, Fig. 4a.[34] Esters **9b** and **10b** were synthesised using a methodology similar to that for **8b** (see ESI†). The cyclisation reaction is expected to be pH sensitive due to the effect of the acid–base equilibrium on the nucleophile. Accordingly, we observed an acceleration of the reaction when the pH increases.[35] Notably, at 37 °C the conversion of **9b** into **12a** occurs rapidly, even under moderate acidic (pH 5, $k_{obs} = 0.65 \pm 0.01 \times 10^{-5}$ s^{-1}) and neutral conditions (pH 7, $k_{obs} = 3.85 \pm 0.05 \times 10^{-5}$ s^{-1}). At pH > 8 the reaction proceeds too rapidly to be accurately measured, Fig. 4b.

§ Amine pK_a values for compounds **5a–7a** and **8b** were obtained by potentiometric titration and data fitting with the Hyperquad2013 program.
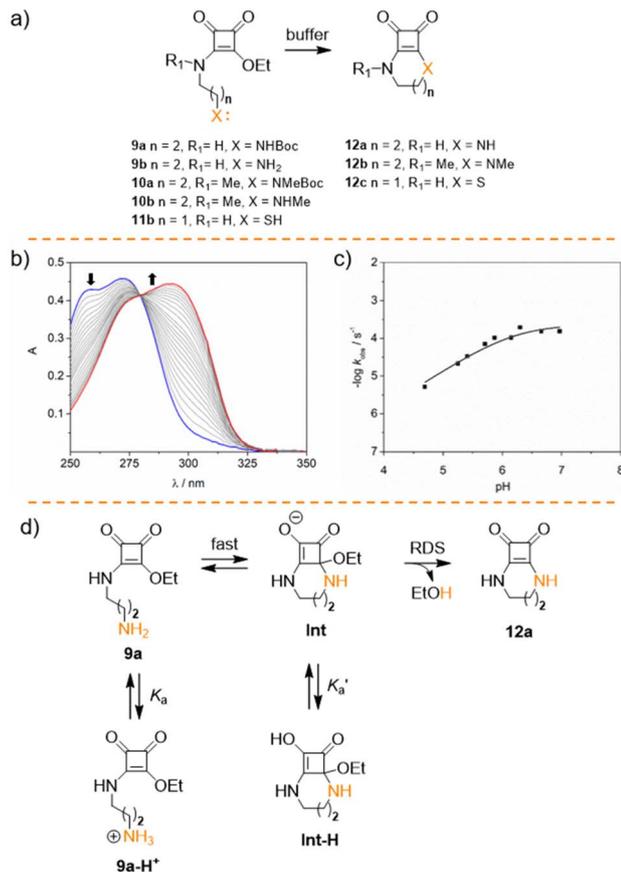
Fig. 4 (a) Structure of the squaramate esters 9a–10c and cyclic compounds 12a–12c. (b) Representative example of the UV changes observed for the cyclisation of 9a (30 μM at 10 mM cacodylate buffer pH 5.7 at 37 °C). (c) Plot of the k_{obs} obtained at pH range 4.5–7. The curve shows the fitting of the experimental data. (d) Proposed intramolecular addition–elimination mechanism for ester 9a to give cyclic squaramide 11a under mildly acidic conditions.

Furthermore, no hydrolytic degradation was observed for the cyclic products 12a and 12b.

Promoting the squaramate ester E,Z conformation significantly affects the cyclization reaction rate. Consequently, the cyclisation reaction accelerates for the N-methylated analogue 10b, becoming too rapid to be accurately measured even at pH 7 by the UV experiments.

To complement the kinetics data for the cyclisation reaction, we studied 9b (30 μM) cyclisation in the pH range of 4.5–7 at 37 °C. As anticipated, plotting the observed rate constants against pH resulted in an asymptotic profile, indicating a strong pH dependence due to the nucleophile sensitivity to pH, Fig. 4c.

The rapid cyclisation of compound 9b hindered the determination of the amine group's pK_a. Homologous compounds of 9b featuring the amino group on shorter alkyl chains have a pK_a around 8.5, as evaluated by potentiometric titration and fitted with Hyperquad (see Fig. S1†). However, within the pH range studied, the amine in compound 9b should be fully protonated, thus behaving as a poor nucleophile and potentially slowing down the formation of the cyclic compound 12a. To address

this, we fitted the kinetic data to obtain the apparent cyclisation kinetic constant k_c and the K_a values using eqn (1). Good fitting was obtained for both constants with $K_a = 6.3 \times 10^{-7}$ (corresponding to a pK_a of 6.2) and $k_c = 2.3 \times 10^{-4}\ s^{-1}$. The calculated pK_a is surprisingly low for an alkylamine. Therefore, we assumed that the obtained K_a represents an apparent acidic constant (K_a') associated with the equilibrium between other species, that determines the reaction rate-determining step (RDS) rather than the nucleophilic amine attack step. Consequently, we propose that the elimination of the leaving group from any tautomeric species with a pK_a of 6.2 becomes the limiting step for this reaction, Fig. 4d. The intermediate species resulting from the rapid intramolecular nucleophilic addition reaction (Int) undergoes a prototropic equilibrium and eliminates an ethanol molecule to facilitate the gain of aromaticity of the tetra-membered ring, to give the cyclic compound. This could be the driving force behind the acidity enhancement of the protonated species up to a pK_a of 6.

To further investigate the effect of the nucleophile nature in the cyclisation reaction kinetics, we synthesised squaramate ester 11b, incorporating a 2-amino ethane thiol as a substituent, Fig. 4a. We hypothesized that the larger size of the sulfur atom would compensate for the shorter length of the alkyl chain and facilitate the formation of the cyclic compound 12c.

Compound 11b was synthetized first by reacting cystamine dihydrochloride with two equivalents of diethyl squarate in acetonitrile in the presence of DiPEA to yield the bis escuaramate ester 11a. Then, before starting the kinetic studies, ester 11b was prepared in situ by reducing 11a with tris(2-carboxyethyl)phosphine (TCEP) (see ESI†).

As anticipated, the UV studies performed with 11b in acidic and neutral buffered solutions (pH 5–7) showed a band at 309 nm corresponding to the tethered cyclothiosquaramide 12c. However, in mild alkaline solutions (pH 8), the 309 nm band diminished over time, and a new band appeared at 332 nm, suggesting the formation of a different product. To elucidate the structure of this unexpected compound, we synthesized the cyclothiosquaramide 12c by reaction of diethyl squarate with cysteamine in a water : ethanol mixture (v/v, 2 : 3). After isolating and characterizing 12c, we let to stand in water at pH 8 (NaOH 1 N) at 50 °C for 5 h to complete its conversion. This yielded a pale yellow solid compound, which was characterised by mass spectrometry and 1D- and 2D-NMR experiments, allowing us to propose the structure of the α-ketocarboxylate 13 shown in Fig. 5a. The transformation of the cyclic compound 12c into the α-ketocarboxylate 13 in alkaline media occurs due to the ring-opening of the cyclobutenedione, provoked by the nucleophilic attack of the hydroxide anion on the C4 carbonyl. The regioselectivity of the ring-opening reaction to yield 13 was confirmed by 2D NMR experiments (see ESI Fig. S12–S17†).

A similar reaction was described by Horri and collaborators for 3,4-diphenylcyclobut-3-ene-1,2-diones, resulting in the formation of the corresponding α-ketoacid.[39]

We used DFT calculations to elucidate why the opening of the four-membered cyclobutadiene-dione ring occurs in compound 12c but not in compounds 12a and 12b at pH ≥ 8. In our computational study, we also included compound 12d to
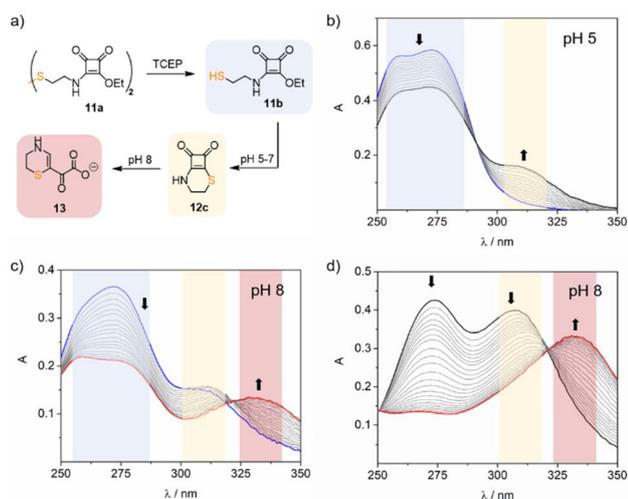
Fig. 5 (a) Synthetic scheme for synthesizing squaramate ester **11a**, cyclothiosquaramide **11c**, and the α-keto carboxylate **13**. UV changes observed for the hydrolysis of **11b** after *in situ* reduction of **11a** at (b) 30 μM, 10 mM acetate buffer, pH 5, 37 °C, and (c) 30 μM, 10 mM PBS buffer, pH 8, 37 °C. (d) UV changes of the degradation of the isolated **12c** at 30 μM, 10 mM PBS buffer, pH 8, 37 °C.

investigate whether the observed experimental differences are attributed to the fused ring size or the presence of the sulfur atom, Fig. 6a.

Remarkably, the energetic profile obtained for the ring opening of compound **12c** upon the addition of the hydroxide anion to the carbonyl differs significantly from that of **12a** or **12d**. That is, for **12c**, the ring opening step has a larger barrier (16.1 kcal mol^{-1}, red profile) than either **12a** (8.5 kcal mol^{-1}, blue profile) or **12d** (10.4 kcal mol^{-1}, yellow profile) Fig. 6b. Additionally, the reaction is exergonic for compound **12c**. Interestingly, for compound **12a**, although the barrier is lower, the resulting opened intermediate is energetically higher
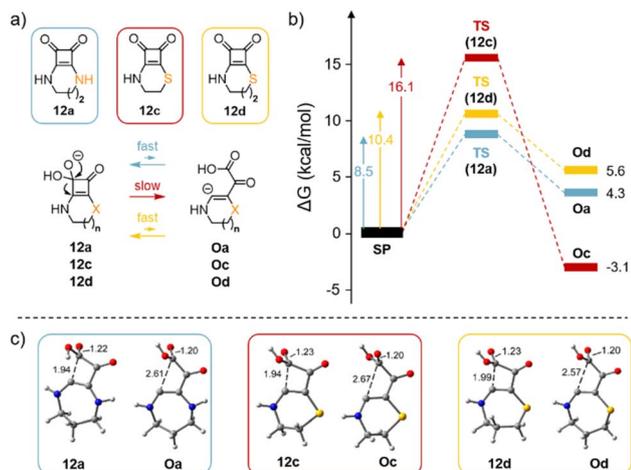

Fig. 6 (a) Cyclobutenediones **12a**, **12c** and **12d**, the reactions studied (1) to (3) and (b) their energetic profiles. (c) The optimised geometries of the transition states and final products are also represented. Distances in Å.

(4.3 kcal mol^{-1}) than the starting product (SP) (blue profile in Fig. 6), thus indicating that any potential fast equilibrium (low barrier) is predominantly shifted towards the starting material. Furthermore, compound **12d** (yellow profile in Fig. 6b) behaves similarly to compound **12a**, suggesting that the ring opening in compound **12c** is likely attributed to the size of the fused ring rather than the presence of the sulphur atom. The geometries of the final products resulting from the opening of the four-membered ring are also represented in Fig. 6c (Oa, Oc and Od). Notably, the carbanion is stabilised by a C($-$)···COOH π-hole interaction.[40] The results align closely with the experimental results as they indicate that only in the case of compound **12c**, the reaction is both exergonic and irreversible.

As observed, the evolution of the squaramate ester **11b** in alkaline media follows a two-step reaction. Firstly, an intramolecular cyclisation yields squaramide thioester **12c**, governed by the cyclisation reaction constant k_c. Secondly, the degradation of **12c** occurs with a pH-dependent rate constant k_{OH}. To investigate this, compound **11b** was studied in the pH range of 3 to 9 at 37 °C, monitoring the spectral UV changes registered upon time to define k_c and k_{OH}.

The formation of the α-ketocarboxylate **13** was not detected at pH 3 and 5. However, in neutral and alkaline media, the reaction rate increased from pH 7 (k_{obs} 0.74 ± 0.05 × 10^{-5} s^{-1}) to pH 9 (k_{obs} 33.4 ± 0.7 × 10^{-5} s^{-1}) as expected. The obtained k_{obs} values exhibited a linear dependence on the hydroxide ion concentration. Using this correlation, we determined the corresponding pseudo-first-order rate constant for the reaction as $k_{OH} = 33.5 ± 0.7$ M^{-1} s^{-1} for the reaction (see ESI eqn (2′)†).

In addition, we calculated the apparent cyclisation rate constant k_c for each studied pH, incorporating the observed k_{OH}, to fit the experimental data. Results indicate that the cyclisation rate increases with the pH, ranging from 0.72 ± 0.02 × 10^{-5} s^{-1} at pH 3 to 16.1 ± 0.3 × 10^{-5} s^{-1} at pH 8. However, the lower value of the k_c (1.23 ± 0.02 × 10^{-5} s^{-1}) at pH 9 suggests that the cyclisation slows down at this pH compared with pH 8, consistent with significant competition from squaramate hydrolysis. By calculating the apparent rate constants k_c we were able to simulate the distribution and evolution of the three species: the squaramide thioester **11b**, the cyclic compound **12c**, and the α-ketocarboxylate **13** over time. For example, at pH 8, ester **11b** rapidly transforms to form the cyclic intermediate **12c** reaching the maximum concentration after 3 h, corresponding to a molar fraction of 0.6. Within approximately 20 hours, the cyclic compound is fully converted into α-keto-carboxylate **13**.

Conclusions

In summary, the squaramate esters investigated in this study exhibit a strong relationship between the alkyl chain nature and their inherent stability in water at 37 °C. Squaramate esters **1a–4a** laking o featuring weak basic NGP groups substitutions remain stable up to pH 9, beyond which hydrolysis becomes significant. The hydrolytic degradation of these compounds ($k_{OH} \approx 10^{-1}$ M^{-1} s^{-1}) is 1000-fold faster than the corresponding rate for squaramides, and follows a conventional second-order

rate law, with a linear dependency on the hydroxide species concentration. Conversely, squaramate esters **5a–7a** and **8b**, functionalised with basic NGP groups such as amines, showed a pH-dependent hydrolysis rate, influenced by the anchimeric assistance of the terminal amino group on the alkyl chain. This mechanism coexists with direct hydroxide hydrolysis reducing their hydrolytic stability to pH 5. However, in squaramate esters **9b–11b** having a terminal nucleophilic group on a sufficiently long alkyl chain, the undergo hydrolysis is overridden by a rapid intramolecular cyclization reaction, resulting in the formation of the corresponding cyclic squaramides **12a–12b** and squaramide-thioester **12c**. Hence, the structure of squaramate and the nature of nearby groups significantly influence their stability in water, thereby affecting their reactivity towards nucleophiles.

Data availability

The authors confirm that the data supporting the findings of this study are available within the article and its ESI.†

Author contributions

Marta Ximenis (conceptualization, investigation); Santiago Canellas (investigation); Rosa M. Gomila (computational studies), Bartomeu Galmés (investigation), Antonio Frontera (supervision), Antonio Costa (supervision), Carmen Rotger (supervision, writing and editing).

Conflicts of interest

There are no conflicts to declare.

Acknowledgements

Notes and references

1 L. F. Tietze, M. Arlt, M. Beller, K. -H. Gl üsenkamp, E. Jähde and M. F. Rajewsky, Anticancer agents, 15. Squaric acid diethyl ester: a new coupling reagent for the formation of drug biopolymer conjugates. Synthesis of squaric acid ester amides and diamides, *Chem. Ber.*, 1991, **124**, 1215–1221.

2 L. F. Tietze, C. Schroter, S. Gabius, U. Brinck, A. Goerlach-Grawj and H.-J. Gabius, Conjugation of p-Aminophenyl glycosides with squaric acid diester to a carrierprotein and use of neoglycoprotein in the histochemical detection of lectins, *Bioconjugate Chem.*, 1991, **2**, 148–153.

3 M. Ávila-Costa, C. L. Donnici, J. D. dos Santos, R. Diniz, A. Barros-Barbosa, A. Cuin and L. F. C. de Oliveira, Synthesis, vibrational spectroscopy and X-ray structural characterization of novel NIR emitter squaramides, *Spectrochim. Acta, Part A*, 2019, **223**, 117354–117366.

4 T. S. Jarvis, C. G. Collins, J. M. Dempsey, A. G. Oliver and B. D. Smith, Synthesis and structure of 3,3-dimethylindoline squaraine rotaxanes, *J. Org. Chem.*, 2017, **82**, 5819–5825.

5 Y. Chen, Y. Li, X. Gao and M. Cui, Squaraine dye based prostate-specific membrane antigen probes for near-infrared fluorescence imaging of prostate cancer, *Dyes Pigm.*, 2022, **208**, 110822–110830.

6 J. Alemán, A. Parra, H. Jiang and K. A. Jørgensen, Squaramides: bridging from molecular recognition to bifunctional organocatalysis, *Chem.–Eur. J.*, 2011, **17**, 6890–6899.

7 F. R. Wurm and H. A. Klok, Be squared: expanding the horizon of squaric acid-mediated conjugations, *Chem. Soc. Rev.*, 2013, **42**, 8220–8236.

8 M. N. Piña, B. Soberats, C. Rotger, P. Ballester, P. M. Deyà and A. Costa, Selective sensing of competitive anions by non-selective hosts: The case of sulfate and phosphate in water, *New J. Chem.*, 2008, **32**, 1919–1923.

9 C. López, E. Sanna, L. Carreras, M. Vega, C. Rotger and A. Costa, Molecular recognition of zwitterions: enhanced binding and selective recognition of miltefosine by a squaramide-based host, *Chem.–Asian J.*, 2013, **8**, 84–87.

10 R. Prohens, G. Martorell, P. Ballester and A. Costa, A squaramide fluorescent ensemble for monitoring sulfate in water, *Chem. Commun.*, 2001, 1456–1457.

11 D. Jagleniec, Ł. Dobrzycki, M. Karbarz and J. Romański, Ion-pair induced supramolecular assembly formation for selective extraction and sensing of potassium sulfate, *Chem. Sci.*, 2019, **10**, 9542–9547.

12 J. Zhou, H. Lin, X. F. Cheng, J. Shu, J. H. He, H. Li, Q. F. Xu, N. J. Li, D. Y. Chen and J. M. Lu, Ultrasensitive and robust organic gas sensors through dual hydrogen bonding, *Mater. Horiz.*, 2019, **6**, 554–562.

13 L. A. Marchetti, T. Krämer and R. B. P. Elmes, Amidosquaramides - a new anion binding motif with pH sensitive anion transport properties, *Org. Biomol. Chem.*, 2022, **20**, 7056–7066.

14 G. Picci, M. Kubicki, A. Garau, V. Lippolis, R. Mocci, A. Porcheddu, R. Quesada, P. C. Ricci, M. A. Scorciapino and C. Caltagirone, Simple squaramide receptors for highly efficient anion binding in aqueous media and transmembrane transport, *Chem. Commun.*, 2020, **56**, 11066–11069.

15 I. Marques, P. M. R. Costa, M. Q. Miranda, N. Busschaert, E. N. W. Howe, H. J. Clarke, C. J. E. Haynes, I. L. Kirby, A. M. Rodilla, R. Pérez-Tomás, P. A. Gale and V. Félix, Full elucidation of the transmembrane anion transport mechanism of squaramides using: In silico investigations, *Phys. Chem. Chem. Phys.*, 2018, **20**, 20796–20811.

16 L. Q. Deng, Y. M. Lu, C. Q. Zhou, J. X. Chen, B. Wang and W. H. Chen, Synthesis and potent ionophoric activity of a squaramide-linked bis(choloyl) conjugate, *Bioorg. Med. Chem. Lett.*, 2014, **24**, 2859–2862.

17 N. Busschaert, I. L. Kirby, S. Young, S. J. Coles, P. N. Horton, M. E. Light and P. A. Gale, Squaramides as potent transmembrane anion transporters, *Angew Chem. Int. Ed. Engl.*, 2012, **51**, 4426–4430.

18 P. Villalonga, S. Fernández de Mattos, G. Ramis, A. Obrador-Hevia, A. Sampedro and C. R. A. Costa, Cyclosquaramides as kinase inhibitors with anticancer activity, *ChemMedChem*, 2012, **7**, 1472–1480.

19 F. Olmo, C. Rotger, I. Ramírez-Macías, L. Martínez, C. Marín, L. Carreras, K. Urbanová, M. Vega, G. Chaves-Lemaur, A. Sampedro, M. J. Rosales, M. Sánchez-Moreno and A. Costa, Synthesis and biological evaluation of N,N'-squaramides with high in vivo efficacy and low toxicity: toward a low-cost drug against Chagas disease, *J. Med. Chem.*, 2014, **57**, 987–999.

20 A. Sampedro, R. Villalonga-Planells, M. Vega, G. Ramis, S. Fernández de Mattos, P. Villalonga, A. Costa and C. Rotger, Cell Uptake and Localization Studies of Squaramide Based Fluorescent Probes, *Bioconjugate Chem.*, 2014, **25**, 1537–1546.

21 V. Molodtsov, P. R. Fleming, C. J. Eyermann, A. D. Ferguson, M. A. Foulk, D. C. McKinney, C. E. Masse, E. T. Buurman and K. S. Murakami, X-ray Crystal Structures of Escherichia coli RNA Polymerase with Switch Region Binding Inhibitors Enable Rational Design of Squaramides with an Improved Fraction Unbound to Human Plasma Protein, *J. Med. Chem.*, 2015, **58**, 3156–3171.

22 L. A. Marchetti, L. K. Kumawat, N. Mao, J. C. Stephens and R. B. P. Elmes, The versatility of squaramides: from supramolecular chemistry to chemical biology, *Chem*, 2019, **5**, 1398–1485.

23 S. Böcker, D. Laaf and L. Elling, Galectin binding to neo-glycoproteins: LacDiNAc conjugated BSA as ligand for human galectin-3, *Biomolecules*, 2015, **5**, 1671–1696.

24 H. Kunz, S. Dziadek, S. Wittrock and T. Becker, Synthetic glycopeptides for the construction of anticancer vaccines, in *Carbohydrate-based Vaccines*, ed. R. Roy, ACS Symposium Series, 2008, vol. 989, pp. 293–310.

25 A. Bergh, B. G. Magnusson, J. Ohlsson, U. Wellmar and U. J. Nilsson, Didecyl squarate - A practical amino-reactive cross-linking reagent for neoglycoconjugate synthesis, *Glycoconjugate J.*, 2002, **18**, 615–621.

26 P. Sejwal, Y. Han, A. Shah and Y. Y. Luk, Water-driven chemoselective reaction of squarate derivatives with amino acids and peptides, *Org. Lett.*, 2007, **9**, 4897–4900.

27 D. Cui, D. Prashar, P. Sejwal and Y.-Y. Luk, Water-driven ligations using cyclic amino squarates: a class of useful SN1-like reactions, *Chem. Commun.*, 2011, **47**, 1348–1350.

28 M. Ximenis, E. Bustelo, A. G. Algarra, M. Vega, C. Rotger, M. G. Basallote and A. Costa, Kinetic analysis and mechanism of the hydrolytic degradation of squaramides and squaramic acids, *J. Org. Chem.*, 2017, **82**, 2160–2170.

29 A. Chernyak, A. Karavanov, Y. Ogawa and P. Kováč, Conjugating oligosaccharides to proteins by squaric acid diester chemistry: Rapid monitoring of the progress of conjugation, and recovery of the unused ligand, *Carbohydr. Res.*, 2001, **330**, 479–486.

30 Y. Shalitin and S. A. Bernhard, Neighboring group effects on ester hydrolysis. I. Neighboring hydroxyl groups, *J. Am. Chem. Soc.*, 1964, **86**, 2291–2292.

31 Y. Shaltin and S. A. Berhard, Neighboring group effects on ester hydrolysis. II. Neighboring carbonyl groups, *J. Am. Chem. Soc.*, 1964, **86**, 2292.

32 J. R. Yerabolu, C. L. Liotta and R. Krishnamurthy, Anchimeric-assisted spontaneous hydrolysisof cyanohydrins under ambient conditions: implicationsfor cyanide-initiated selective transformations, *Chem.–Eur. J.*, 2017, **23**, 8756–8765.

33 J. L. García Ruano, A. M. Martín Castro and J. H. Rodriguez Ramos, Anchimeric assistance of the sulfinyl group in the hydrolysis of cyano groups: a new mild method for the reduction of sulfoxides, *Tetrahedron Lett.*, 1996, **37**, 4569–4572.

34 M. Ximenis, J. Piterch-Jarque, S. Blasco, C. Rotger, E. García-España and A. Costa, Water-soluble squaramide dihydrates: N-methylation modulates the occurrence of one- and two-dimensional water clusters through hydrogen bonding and dipolar interactions, *Cryst. Growth Des.*, 2018, **18**, 4420–4427.

35 M. Ximenis, A. Sampedro, L. Martínez-Crespo, G. Ramis, F. Orvay, A. Costa and C. Rotger, Introducing a squaramide-based self-immolative spacer for controlled drug release, *Chem. Commun.*, 2021, **57**, 2736–2739.

36 K. Covington, M. I. A. Ferra and R. A. Robinson, Ionic product and enthalpy of ionization of water from electromotive force measurements, *J. Chem. Soc., Faraday Trans. 1*, 1977, **73**, 1721–1730.

37 P. F. Fitzpatrick, Combining solvent isotope effects with substrate isotope effects in mechanistic studies of alcohol and amine oxidation by enzymes, *Biochim. Biophys. Acta*, 2015, **1854**, 1746–1755.

38 P. Yurkanis Bruice and H. G. Mautner, Intramolecular catalysis and the involvement of tetrahedral intermediate partitioning in the hydrolysis of benzoylcholine, benzoylthionocholine, and their dimethylamino analogs, *J. Am. Chem. Soc.*, 1973, **95**, 1582–1585.

39 A. Al-Najjar, K. Bowden and M. V. Horri, Reactions of carbonyl compounds in basic solutions. Part 25.1 The mechanism of the base-catalysed ring fission of 3,4-diphenylcyclobut-3-ene-1,2-diones, *J. Chem. Soc., Perkin Trans.*, 1997, **2**, 993–996.

40 J. S. Murray, P. Lane, T. Clark, K. E. Riley and P. Politzer, σ-Holes, π-holes and electrostatically-driven interactions, *J. Mol. Model.*, 2012, **18**, 541–548.